Proceedings World Geothermal Congress 2020+1
Reykjavik, Iceland, April - October 2021

Scale Inhibitors for Metal Silicate Fouling

Konstantinos D. Demadis,[1] Argyro Spinthaki,[1] Michaela Kamaratou,[1] Juergen Matheis,[1] Duygu Disci-Zayed,[1] and Wolfgang Hater[1]

[1]Crystal Engineering, Growth and Design Laboratory, Department of Chemistry, University of Crete, Voutes, Heraklion, Crete, GR-71003, Greece

[2]Kurita Europe GmbH, Giulinistrasse 2, 67065 Ludwigshafen, Germany

demadis@uoc.gr

Keywords: silica, metal silicates, deposits, magnesium, aluminum.

ABSTRACT

Deposits appearing in industrial water processes and contain both "metal ions" and "Si", are usually referred to as "metal silicates". However, this general aphorism is not correct, because these precipitates rarely resemble their well-characterized geological counterparts. In the present paper the focus is on water-formed precipitates that contain two components, "metal ions" (Mg or Al) and "silicate". Efforts were put forth in an attempt to delineate the true nature of such Mg-, Al- and Si-containing precipitates formed under the severe stresses simulating geothermal-like conditions. The purpose of this work is to deliberately form precipitates in the presence of Mg^{2+} or Al^{3+} ions and soluble silica (silicic acid) and study these with a variety of analytical techniques, to reveal morphology, texture, structure and composition. Such precipitates are better described as "magnesium (or aluminum)-containing amorphous silica".

Furthermore, inhibition experiments were carried out in supersaturated solutions of different silicate and magnesium or aluminum concentrations at pH values from 7.0 up to 10.0. Anionic additives were found to act as stabilizing agents probably by complexing the magnesium or aluminum cations, and thus preventing "magnesium/aluminum silicate" formation. Based on a plethora of experimental data, a number of useful functional insights have been generated, which add to building a more complete and comprehensive picture of the mechanism of "metal silicate" formation and inhibition/stabilization.

1. INTRODUCTION

Metal silicates form in process waters with high silica and polyvalent metal ion content (Demadis 2010, Gallup and von Hirtz 2015). Such precipitates/deposits are common in geothermal installations, depending on the particular brine chemistry. Iron and magnesium silicates exhibit low solubility in brines with low enthalpy (Topçu *et al.* 2017), while aluminum silicate usually precipitates in fluids of higher temperatures (Kristmannsdottir 1989).

Although the term "magnesium silicate" is well recognized in the water treatment industry, its precise definition is different from that in geochemistry. The identity of the "magnesium silicate" scales in the water treatment industry remains poorly-defined in contrast to the geological minerals with well-defined structures and properties. It is common to call any deposit that contains "Mg" and "Si" as "magnesium silicate". The "magnesium silicate" system, much like the amorphous silica system (with no metals present), is strongly pH-dependent. "Magnesium silicate" precipitation practically does not occur at pH regions < 8.5. In addition its tendency to precipitate is enhanced as pH increases, see Figure 1.

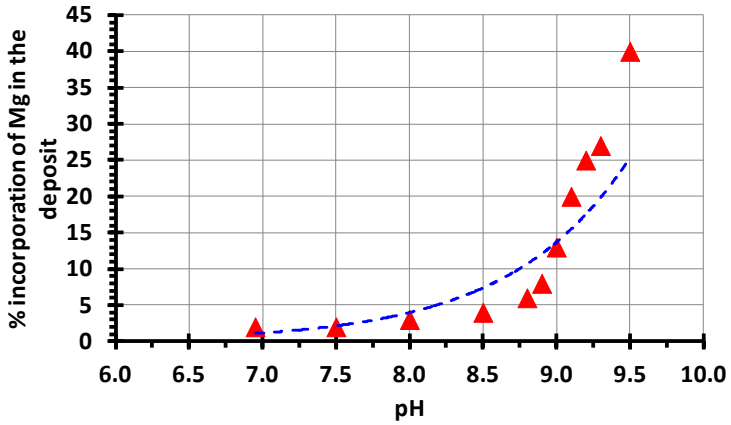

Figure 1: The effect of pH on the precipitation of magnesium silicate.

An explanation for this phenomenon is the enhanced deprotonation of monomeric silicic acid $[Si(OH)_4]$ in pH regions, that yields silicate ions $[Si(OH)_3O^-]$. These interact with dissolved Mg^{2+} cations via electrostatic interactions. In pH regimes < 7 magnesium silicate does not form, and the only chemistry occurring is the polycondensation of silicic acid to form colloidal silica (Mavredaki *et al.* 2005, Ketsetzi *et al.* 2008, Stathoulopoulou and Demadis 2008, Hater *et al.* 2013). Previous studies from our laboratory have revealed that dissolved Mg^{2+} cations act as catalysts in silica polycondensation chemistry (Demadis *et al.* 2012, Demadis 2003). Another controversial topic is the Mg:Si atom ratio in the formed "magnesium silicate" precipitates. Previously, it was suggested

that the ratio is 1:1, but shows some variation (Young 1993). Later, other researchers proposed different ratios, such as 1:2, 1:5, 1:10 and even 1:20. Therefore, the issue is still controversial (Kristmanndóttir *et al.* 1989). An important fact is that this scale is amorphous and it is not recognized as a member of the extensive magnesium silicate mineral family.

Deposit removal from industrial equipment include mechanical (Arata *et al.* 1999) and chemical cleaning (Deutscher *et al.* 1980), or a combination of both (Messer *et al.* 1978). Both require operational shut-downs. Scale control methods such as hot brine reinjection (Henley 1983), and adjustment of brine pH (Rothbaum *et al.* 1979) have been evaluated. Brine acidification has been successfully applied in some cases, however, metallic corrosion, cost of acids and human safety risks become important issues (Gallup 1996). Hence, scale control by chemical inhibitors may be a preferable way forward.

Development and successful application of scale inhibitors require advanced understanding of the mechanism of scale formation as well as its compositional and chemical identity. Recently, studies on the formation and characterization of "magnesium silicate" precipitates/deposits under geothermal stresses were reported by our group (Spinthaki *et al.* 2018). Process variables evaluated were: (a) Mg^{2+} concentration, (b) silicate concentration, (c) pH, and (d) temperature. Important conclusions drawn were: (a) precipitate formation is pH-dependent (as pH increases, the precipitation driving force increases), (b) precipitation is more pronounced with increased silicate and Mg^{2+} concentrations, (c) all precipitates were amorphous, (d) Mg elemental distribution within the isolated precipitates was random (pointing to a non-stoichiometric precipitation process), and (e) temperature-dependence of precipitation is rather insignificant. Based on those results, it was proposed that the most accurate technical term to describe the inorganic precipitates formed under certain experimental conditions (in the presence of Mg^{2+} and silicate at pH 10) is "magnesium-containing amorphous silica".

Similar arguments can be put forth for "aluminum silicate" precipitates. "Aluminum silicate" typically precipitates at pH from 4 to 10 although the rate of precipitation increases at regions pH > 9 and decreases in pH regime 5-8. Importantly, "aluminum silicate" tends to precipitate at a higher temperatures than those for amorphous silica (Gallup 1997). Water chemistries (such as that in the Salton Sea) have provided evidence that low concentrations of Al^{3+} can cause precipitation, and it is found at higher levels in formed scales (Gallup 1998). It is widely accepted that the speciation of Al^{3+} in aqueous systems is very complex. This is the major reason why "aluminum silicate" scales identified in water-related industries are heterogeneous in composition. They demonstrate physicochemical features different than those of the geological minerals (Canizares *et al.* 2006, Perry and Shafran 2001). In precipitates obtained from several geothermal plants, Al:Si ratios are non-stoichiometric and vary from 1:8, 1:10, 1:20 and even 1:40. The most reasonable scenario that can be drawn, consistent with the data, is that Al^{3+} is incorporated in, or adsorbed onto the amorphous silica matrix, and in certain cases, it catalyzes the silica polycondensation process (Browne and Driscoll 1992). Another scenario is that aluminum hydroxide adsorbs high concentrations of silicic acid, a hypothesis that applies for Fe^{3+} present in the brine (Yokoyama *et al.* 1993).

Herein, we describe in detail the influence of five commercially-available phosphonates on the precipitation of sparingly-soluble materials that separate out of solution in the presence of Mg^{2+} or Al^{3+} ions and soluble silica (silicic acid). These phosphonates are PBTC, HEDP, AMP, HDTMP, and BHMTPAMP and their chemical structures are presented in Figure 2.

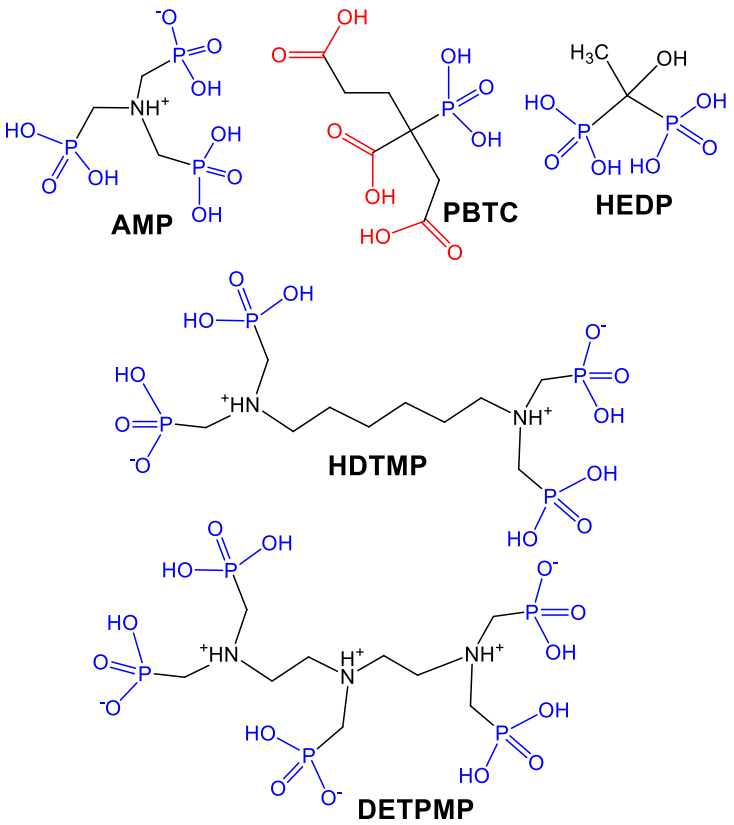

Figure 2: Schematic structures of the chemical additives used in this study with their abbreviated names. Phosphonate groups are shown in blue, carboxylate ones in red.

2. EXPERIMENTAL SECTION

2.1 Instrumentation

ATR-IR spectra were collected on a Thermo-Electron NICOLET 6700 FTIR optical spectrometer. Measurements of soluble silicic acid (molybdate-reactive silica) were carried out using a HACH 1900 spectrophotometer from the Hach Co., Loveland, CO, USA.

2.2 Reagents and Materials

All chemicals were from commercial sources and were used as received, witout further purification. Phosphonate additives (Figure 1) were members of the Dequest® series supplied by ThermPhos Inc. (acquired by Italmatch), with the following commercial names: PBTC Dequest 7000, HEDP Dequest 2010, AMP Dequest 2000, HDTMP Dequest 2054, and BHMTPAMP Dequest 2090. Sodium silicate $Na_2SiO_3 \cdot 5H_2O$, ammonium molybdate ($(NH_4)_6Mo_7O_{24} \cdot 4H_2O$), sodium hydroxide (NaOH) and oxalic acid ($H_2C_2O_4 \cdot 2H_2O$) were from EM Science (Merck). Aluminium chloride hexahydrate ($AlCl_3 \cdot 6H_2O$), hydrochloric acid 37% and magnesium chloride hexahydrate ($MgCl_2 \cdot 6H_2O$) were from Riedel de Haen. Ethylenediamine tetraacetic acid (EDTA, tetrasodium salt) and Eriochrome Black T were from Alfa Aesar. Sulfuric acid 95-97 % (H_2SO_4) and L-Ascorbic acid 99 % ($C_6H_8O_6$) were purchased from Sigma Aldrich. Sodium acetate ($NaC_2H_3O_2 \cdot 3H_2O$) was from Fluka. Analytical grade glacial acetic acid was from Scharlau. Eriochrome Cyanine R was from Alfa Aesar. All reagents were used as received from suppliers, without further purification. Acrodisc filters (porosity 0.45 μm) were from Pall-Gelman Corporation. In-house, deionized (DI) water was used for all experiments. This water was tested for soluble silica and magnesium ions and was found to contain negligible amounts. The protocols followed herein have been previously reported in detail (Spinthaki *et al.* 2018). Experiments were carried out either at 25 °C, or under hydrothermal conditions (200 °C), under autogenous pressure. Precipitation reactions were carried out at pH 10.0. Polyethylene (PET) containers were exclusively used to avoid silicate leaching from glass. Molybdate-reactive silicic acid was measured using the silicomolybdate spectrophotometric method (± 5 % precision) with excellent reproducibility (Truesdale *et al.* 1979).

2.3 Stock Solution Preparation

The sodium silicate stock solution (*solution A*) used in all experiments was prepared by dissolving 4.080 g of $Na_2SiO_3 \cdot 5H_2O$ in 2 L DI water to obtain 500 ppm (8.33 mM) SiO_2. The mixture was stirred for at least a day to ensure complete dissolution. A 1 % w/v (10,000 ppm in Mg^{2+}) solution (*solution B*) was prepared by dissolving 8.360 g of $MgCl_2 \cdot 6H_2O$ in 100 mL DI water. A 0.01 M Na_4EDTA solution (*solution C*) was prepared by dissolving 1.900 g of Na_4EDTA in 500 mL DI water. The ammonium molybdate solution (*solution D,* kept in the refrigerator) used in the silicomolybdate test was prepared by dissolving 10 g $(NH_4)_6Mo_7O_{24} \cdot 4H_2O$ in 100 mL DI water, to which 24 pellets of solid NaOH were added under stirring, followed by pH adjustment to 7.7-7.8. A HCl stock solution (*solution E*) was prepared by mixing equal quantities of concentrated HCl (37% w/v) and DI water. The oxalic acid solution (*solution F*) was prepared by dissolving 8.750 g of solid hydrated oxalic acid, $H_2C_2O_4 \times 2H_2O$, in 100 mL DI water. A 1 % w/v Eriochrome Black T solution (*solution G*) was prepared by dissolving 0.30 g in 30 mL ethanol. Stock solutions of 10,000 ppm (as actives) of each phosphonate were also prepared (*solutions H*). A 1 % w/v (10,000 ppm in Al^{3+}) solution (*solution I*) was prepared by dissolving 8.440 g of $AlCl_3 \cdot 6H_2O$ in 100 mL DI water. Sulfuric acid (H_2SO_4) 0.02 N (*solution J*) was prepared by 25 mL pure sulfuric acid diluted in 25 mL of deionized H_2O. This results in a 1:1 sulfuric acid solution. From this 1:1 sulfuric acid solution, 0.0533 mL was diluted in deionized H_2O to a final volume of 50 mL. 68 g sodium acetate (*solution K*, buffer solution) was dissolved in 200 mL deionized water. Then 1.144 mL of glacial acetic acid was added to the solution. The solution was then diluted with DI water to a volume of 500 mL. Ascorbic acid (*solution L*, prepared daily) was prepared by dilution of 25 mg of solid reagent in 25 mL of DI H_2O. Eriochrome cyanine R (*solution M*) was prepared by diluting 0.015 g in 5 mL of DI H_2O. The solution's pH was adjusted to 2.9 by using acetic acid, diluted in deionized H_2O in equal volumes. Deionized water was added until the final volume of 100 mL.

2.4 Precipitate Formation in the Presence of Mg^{2+} and Silicate (Control)

A quantity of silicate solution A (10 mL) was placed in a PET container. The pH of this solution was initially ~12.0, hence, to avoid magnesium hydroxide precipitation, adjustment to pH < 9.5 was necessary. The desired volumes of the treatment solution (solutions H), then Mg solution (B) were placed in the container. The desired pH of 10.0 was achieved by addition of HCl solution (E). Further pH adjustment was done by a solution of NaOH if needed. The necessary amount of the 1% w/v (10,000 ppm in Mg^{2+}, solution B) was used (0.50 mL), such that the final Mg^{2+} concentration was 200 ppm (as Mg). The volume of the combined solution A+B is made up to 25 mL. The final working solution contained 200 ppm silicic acid (as SiO_2) and 200 ppm of Mg^{2+} (as Mg). Finally, the container was covered with plastic membrane and set aside without stirring. The solutions were checked for soluble silicic acid by the silicomolybdate yellow method (see below) every half hour for the first hour and every hour for the next three hours after the final pH adjustment (t = 0). In all results presented below the concentration of molybdate-reactive silica is expressed as ppm (as SiO_2).

2.5 Effect of Inhibitors on Precipitate Formation in the Presence of Mg^{2+} and Silicate

The same procedure as the control (see above) was followed, except that after pH adjustment to lower values the required amount of inhibitor solution (concentrations of 50, 100, 200, 500, and 1500 ppm) was added *before* addition of solution B. Afterwards, the same procedure described above was followed.

2.6 Precipitate Formation in the Presence of Al^{3+} and Silicate (Control)

The required quantity of 1% Al^{3+} solution (I) was placed in a PET container to target Al^{3+} concentration of 25, 50, 75, 100, 150, 200 and 300 ppm (as Al). The pH of this solution was initially ~4.0. The desired volume of silicic acid solution (A) was placed in the container and the desired pH value was achieved by addition of HCl and NaOH if needed. The volume of the combined solution A+I was made up to 25 mL. The final working solution contains 150 ppm silicic acid (as SiO_2) and the aforementioned variable amounts of Al^{3+}. Finally, the container was covered with a plastic membrane and set aside without stirring. The solutions were checked for soluble silicic acid by the silicomolybdate yellow method (see below) every half hour for the first hour and every hour

for the next three hours after the final pH adjustment (t = 0). In all results presented below the concentration of molybdate-reactive silica is expressed as ppm (as SiO_2).

2.7 Effect of Inhibitors on Precipitate Formation in the Presence of Al^{3+} and Silicate

In general, the same procedure as the control was followed, except that after pH adjustment to lower values the required amount of inhibitor solution (such as concentrations of 50, 100, 200, 500, and 1500 ppm) was added before addition of solution I. After that the same procedure as above was followed.

2.8 Quantification of "Soluble (Molybdate-reactive) Silica"

"Soluble" or "reactive" silica refers to soluble silicic acid and was determined using the "yellow" silicomolybdate spectrophotometric method. According to this method 2 mL of working solution were filtered through a 0.45 μm syringe filter, and diluted to 25 mL in a cell with light path 1 cm. One mL of solution D and 0.5 mL of solution E were added to the sample cell, the solution was mixed well and left undisturbed for 10 min. Then 1 mL of solution F was added and mixed again. The solution was set aside for 2 min. After the second period the photometer was set to zero absorbance with DI water. Finally, the sample absorbance was measured at 452 nm as "ppm soluble silica". The detectable concentrations range is 0 – 75.0 ppm. In order to calculate the concentration in the original solution a dilution factor is applied. The silicomolybdate method is based on the principle that ammonium molybdate reacts with reactive silica, and any phosphate present at low pH (about 1.2) yields heteropoly acids, yellow in color. Oxalic acid is added to destroy the molybdophosphoric acid leaving silicomolybdate intact, and thus eliminating any color interference from phosphates. This method determines "*soluble silica*", a term that includes molybdate-reactive species. Icopini *et al.* (2005) defined "molybdate-reactive" to include the species monomeric (monosilicic acid, H_4SiO_4), dimeric (disilicic acid, $H_6Si_2O_7$), and possibly trimeric ($H_8Si_3O_{10}$) silica. Since trimeric silica has never been detected in any of these or past experiments (Preari *et al.* 2014), the term "molybdate-reactive" silica refers to a mixture of monosilicic acid (primarily) and disilicic acid (to a lesser extent), with the first being dominant under our experimental conditions. Silica, in the monomeric state will react with molybdic acid within the first 75 seconds of contact at 20 ^oC, whereas disilicic acid needs about 10 minutes. Other silica oligomers require longer times to react. It should be noted that Al^{3+} does not interfere with the silicomolybdate spectrophotometric method.

2.9 Quantification of Soluble Mg^{2+}

The Mg^{2+} concentration in the working solutions was determined by the EDTA titrimetric method (Eaton *et al.* 2012). According to this protocol, 1 mL sample of the working solution is diluted to 10 mL with deionized water. The pH is adjusted to ~ 11 with 1.0 N NaOH solution. Then, 3 drops of EBT solution (solution G) are added to the solution. Slow addition of EDTA titrant (solution C) with continuous stirring to the proper end point and calculation of the magnesium concentration follow. Mg^{2+} is expressed in "ppm as Mg".

2.10 Quantification of Soluble Al^{3+}

The Al^{3+} concentration in the working solutions was determined by the Eriochrome Cyanine R Method (Shull and Guthan 1967). According to this method, 3 mL of the working solution is filtered through a 0.45 μm syringe filter. The first 2.5 mL of the filtrate are discarded. The remaining 0.5 mL is used as the sample quantity and is being placed in a cell with light path 1 cm. Different sample quantities are used for different concentrations of Al^{3+}. Then, 0.5 mL of *solution J*, 0.5 mL of *solution L*, 5 mL of *solution K* and 2.5 mL of *solution M* are added in the cell and mixed by shaking. Deionized water is added to a final volume of 25 mL. A similar cell, containing 0.5 mL of *solution J*, 0.5 mL of *solution L*, 5 mL of *solution K* and 2.5 mL *solution M* and diluted to a 25 mL final volume is used as blank. The solution is set aside for 7.5 minutes and finally the absorption at 535 nm, using a DR-1900 spectrophotometer is measured. The accuracy of the method is ± 1.7 %.

3. RESULTS AND DISCUSSION

3.1 Control of "Magnesium Silicate" Formation

In this work, experimental conditions were fixed to $[Mg^{2+}] = [SiO_{2(sol)}] = 200$ ppm ($[Mg^{2+}] = 8.23$ mM, $[SiO_{2(sol)}] = 3.33$ mM) at pH = 10.0. A range of inhibitor concentrations was tested at 50, 100, 200, 500, and 1500 ppm (as actives). Quantification of inhibitor efficiency was based on molybdate-reactive silica and Mg^{2+} and Al^{3+} measurements that remained in solution for 4 hours after the onset of the precipitation reaction. Figure 3 shows results for the lowest (50 ppm) dosage for BHMTPAMP, AMP, HDTMP, PBTC, and HEDP, and as inhibitors. Figure 4 shows results with the highest dosage (1500 ppm).

Based on silica and Mg^{2+} loss in the absence of inhibitors (control, dotted lines), it appears that silica reduction is more pronounced than Mg^{2+} reduction. Silica loss is calculated (based on moles) to be ~ 85 %, and Mg loss is ~ 50 % (Mg:Si ~ 0.6:1.0). This is consistent with the previous observation that very little Mg^{2+} is incorporated in the inorganic precipitate, in Mg:Si molar ratios ranging from 0.2:1.0 to 0.9:1.0, *ie.* in sub-stoichiometric amounts. Even at low inhibitor concentration (50 ppm), scale control is noticeable. Silica (ΔSilica) and Mg (ΔMg) splits gradually increase as inhibitor concentration increases. The term "split" is defined as the actual measurement of either silica or Mg (in ppm) after subtraction of the "control" value. Table 1 summarizes the silica (ΔSilica) and Mg (ΔMg) splits for all inhibitors for the lowest (50 ppm) and highest (1500) dosages. All inhibitors are partially effective in controlling soluble silica at the 50 ppm dosage. The least effective inhibitor is PBTC (4 % stabilization) and the highest control is achieved by HDTMP (27 % stabilization). All inhibitors exhibit variable performance at their highest dosage of 1500 ppm. The least effective inhibitor is BHMTPAMP (45 % stabilization) and the most effective one is PBTC (86 % stabilization). It appears that these phosphonate inhibitors are much more effective in Mg^{2+} stabilization. At the lowest dosage of 50 ppm, the lowest stabilization is exhibited by BHMTPAMP (43 % stabilization) and the highest by HEDP (63 % stabilization). Dosage increasing to 1500 ppm has a profound effect in stabilization efficiency. The highest, and nearly quantitative stabilization is found for both PBTC and BHMTPAMP (96 % stabilization), whereas the lowest for HEDP (47 % stabilization). Dosage increase enhances stabilization, except for Mg^{2+} stabilization by HEDP, for which a drop from 63 % to 47 % is observed in spite of increase in inhibitor dosage.

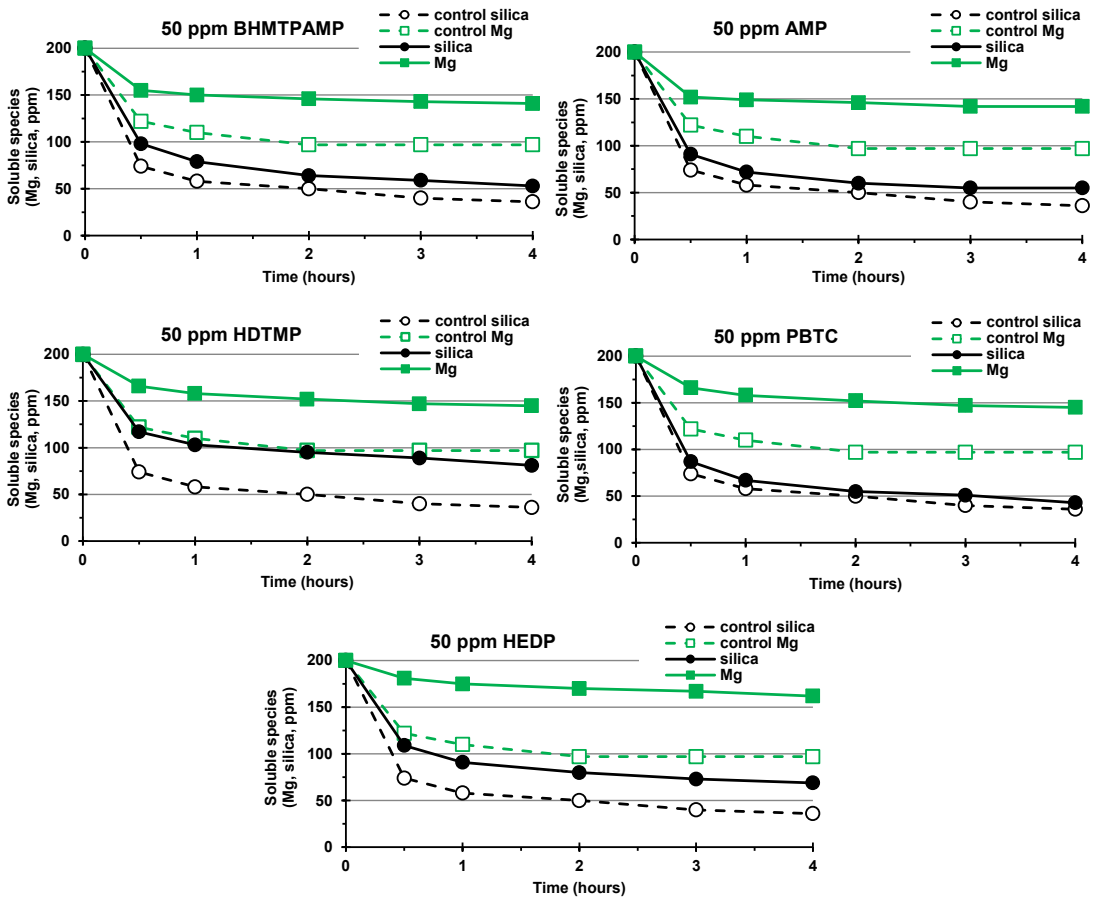

Figure 3: Simultaneous stabilization of Mg2+ and silicate, in the presence of 50 ppm of phosphonate inhibitors. "Control" refers to experiments without antiscalants, whereas "silica" and "Mg" refer to measurements in the presence of inhibitors, as indicated.

Precipitates in the presence of 1500 ppm inhibitor were isolated after 4 hours of precipitation time. They are all amorphous as indicated by powder X-ray diffraction studies (data not shown). No indication for the presence of crystalline magnesium silicates could be derived from the diffraction patterns in agreement with our previous observations. Precipitates were also examined by Scanning Electron Microscopy for morphological features, particle size and agglomeration tendency. Particle morphology is similar in all samples studied displaying the common feature of particle aggregation. This phenomenon seems to be enhanced in precipitates originated from phosphonate-containing solutions compared to precipitates in the absence of inhibitor. It is likely that the phosphonate inhibitor (at least partially) is entrapped within the precipitate matrix. Energy- dispersive X-ray spectroscopy has provided proof for inhibitor entrapment based on the detection of P, which could only originate from the phosphonates. Precipitate samples that were isolated in the presence of any of the inhibitors showed variable, but low Mg:P atomic ratios, close to the value of 12:1. Figure 5 provides elemental mapping for a precipitate that was isolated after 4 hours, in the presence of 1500 ppm of HDTMP inhibitor. Besides the expected presence of Mg and Si, there is also P present that originates from the HDTMP. This points out to two possible events: (a) the phosphonate inhibitor is entrapped into the precipitate, and (b) a possible "Mg-HDTMP" complex co-precipitated with the "Mg-silicate" precipitate. Unfortunately, with the available techniques, it is difficult to distinguish between the two scenarios.

Based on the results presented in Table 1, inhibitor efficiency can be realized with the following ranking (1500 ppm inhibitor dosage).

For silica stabilization: PBTC > HEDP > AMP > HDTMP > BHMTPAMP

For Mg^{2+} stabilization: PBTC = BHMTPAMP > AMP > HDTMP > HEDP

The observed variation in the ranking between silica and Mg^{2+} stabilization is certainly a result of the different mechanisms of stabilization.

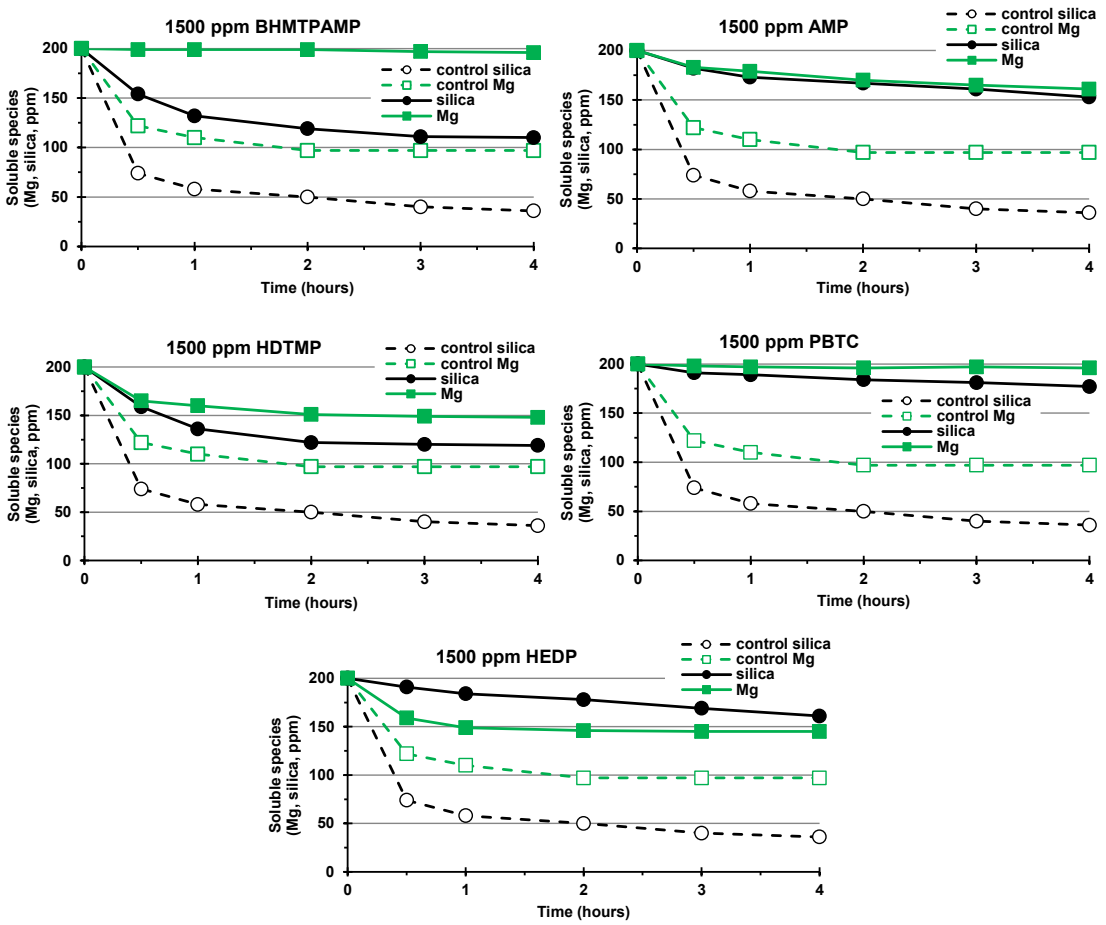

Figure 4: Simultaneous stabilization of Mg^{2+} and silicate, in the presence of 1500 ppm of phosphonate inhibitors.

Table 1: Silica (ΔSilica) and Mg (ΔMg) splits for all inhibitors present in the "magnesium silicate" system after 4 hours of precipitation time.[a]

Inhibitor dosage (ppm)	ΔSilica, ppm				
	PBTC	HEDP	AMP	HDTMP	BHMTPAMP
50	7	33	15	45	17
1500	141	125	117	83	74
	ΔMg, ppm				
	PBTC	HEDP	AMP	HDTMP	BHMTPAMP
50	48	65	45	48	44
1500	99	48	64	51	99

[a] The term "split" is defined as the actual measurement of either silica or Mg^{2+} (in ppm) after subtraction of the "control" value.

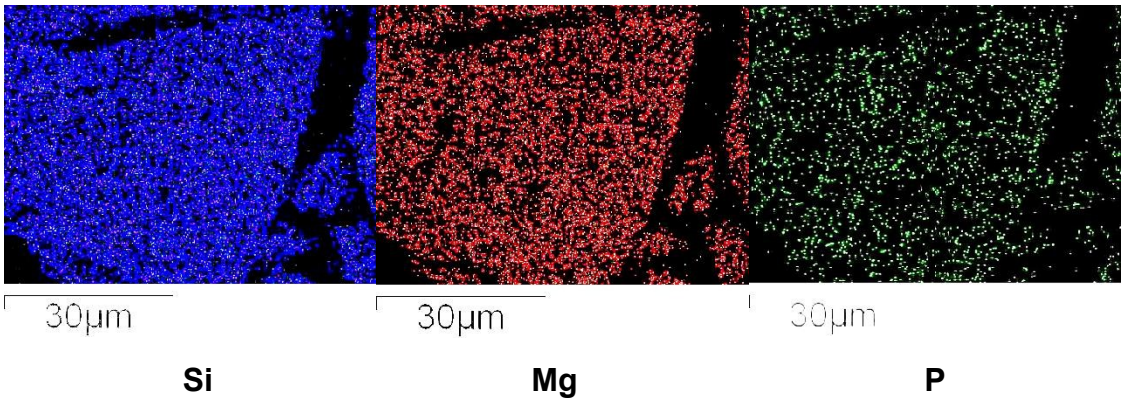

Figure 5: Elemental mapping of "magnesium silicate" precipitates in the presence of 1500 ppm HDTMP inhibitor.

3.2 Control of "Aluminum Silicate" Formation

In this work, experimental conditions were fixed to $[Al^{3+}] = [SiO_{2(sol)}] = 150$ ppm ($[Al^{3+}] = 5.55$ mM, $[SiO_{2(sol)}] = 2.50$ mM) at pH = 10.0, and additive concentration was tested at 50, 100, 200, 500, and 1500 ppm. Quantification of inhibitor efficiency was based on molybdate-reactive silica and soluble Al^{3+} that remained in solution for 3 hours after the onset of the precipitation reaction. Figure 6 shows results for the lowest (50 ppm) dosage for AMP, PBTC, HEDP, BHMTPAMP, and HDTMP as inhibitors. Figure 7 shows results with the highest dosage (1500 ppm). Also, the silica (ΔSilica) splits gradually increase as inhibitor concentration increases. The term "split" is defined as the actual measurement of silica (in ppm) after subtraction of the "control" value. Table 2 summarizes the silica (ΔSilica) splits for all inhibitors for the lowest (50 ppm) and highest (1500) dosages.

At the lowest inhibitor dosage (50 ppm) there is virtually no inhibitory performance. All inhibitors stabilize < 20 ppm silica above the control, therefore they are deemed ineffective at the 50 ppm dosage. At the highest inhibitor dosage (1500 ppm) all additives show variable inhibitory activity. Specifically, PBTC, HEDP, BHMTPAMP and HDTMP stabilize 50-76 ppm silica above the control. AMP is the most efficient antiscalant demonstrating stabilization of 106 ppm above the control. When it comes to Al^{3+} stabilization, all inhibitors stabilize < 2 ppm Al^{3+} above the control, therefore they are deemed ineffective at the 50 ppm dosage. At the highest inhibitor dosage (1500 ppm) only the PBTC additive shows mediocre inhibitory activity, stabilizing 38 ppm Al^{3+} above the control.

Precipitates in the absence or presence of 1500 ppm inhibitor were isolated after 3 hours of precipitation time. They are all amorphous as indicated by powder XRD studies (data not shown). No indication for the presence of crystalline aluminum silicates could be derived from the diffraction patterns. EDS results showed a sub-stoichiometric Al:Si ratio 0.55.

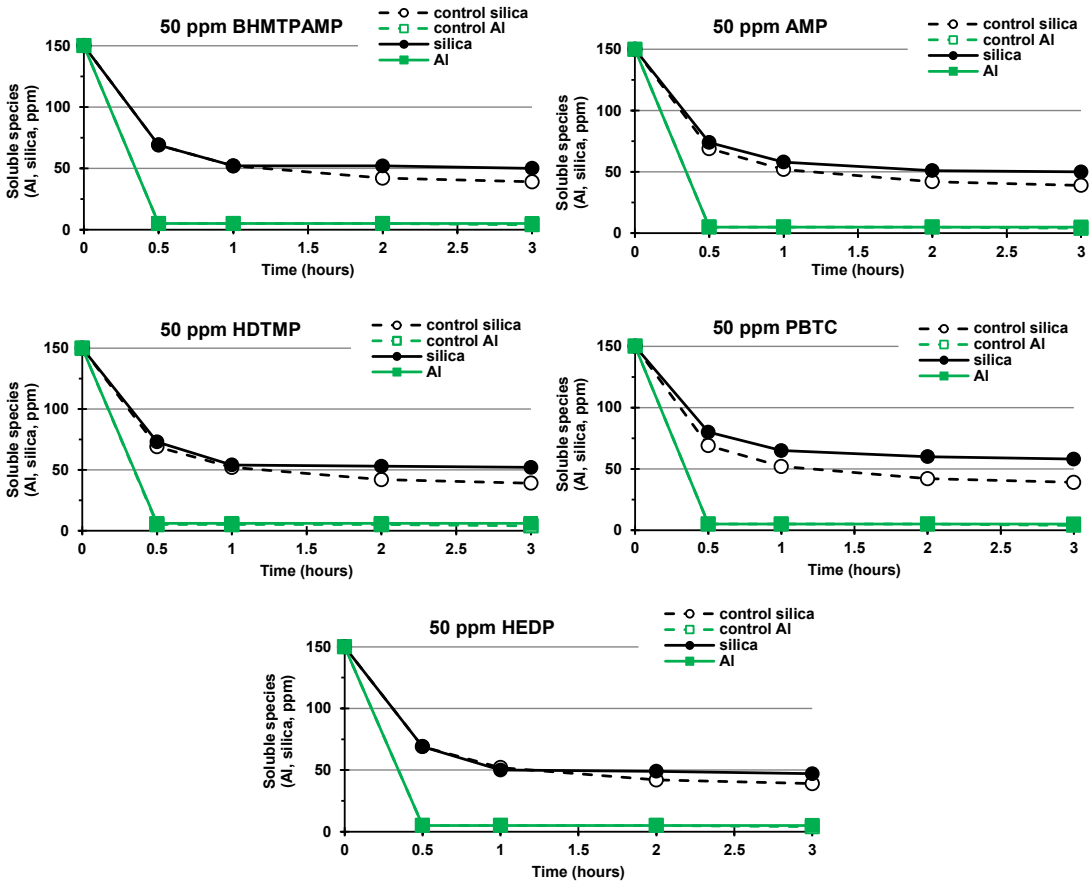

Figure 6: Simultaneous stabilization of Al^{3+} and silicate, in the presence of 50 ppm of phosphonate inhibitors. "Control" refers to experiments without antiscalants, whereas "silica" and "Al" refer to measurements in the presence of inhibitors, as indicated.

Based on the results presented in Table 2, inhibitor efficiency in the Al-silica system can be realized with the following ranking (1500 ppm inhibitor dosage).

For silica stabilization: AMP > BHMTPAMP > HDTMP > PBTC > HEDP

For Al^{3+} stabilization: PBTC > BHMTPAMP > HDTMP > HEDP > AMP

The observed variation in the ranking between the Mg-silica and Al-silica systems is certainly a result of the different stabilization mechanisms.

Figure 8 provides elemental mapping for a precipitate that was isolated after 3 hours, in the presence of 1500 ppm of HDTMP inhibitor. Besides the expected presence of Al and Si, there is also P present that originates from the HDTMP. This points to two possible events occurring simultaneously: (a) the phosphonate inhibitor is entrapped into the precipitate, and (b) a possible "Al-

HDTMP" complex co-precipitated with the "Al-silicate" precipitate. Unfortunately, with the available techniques, it is difficult to distinguish between the two scenarios.

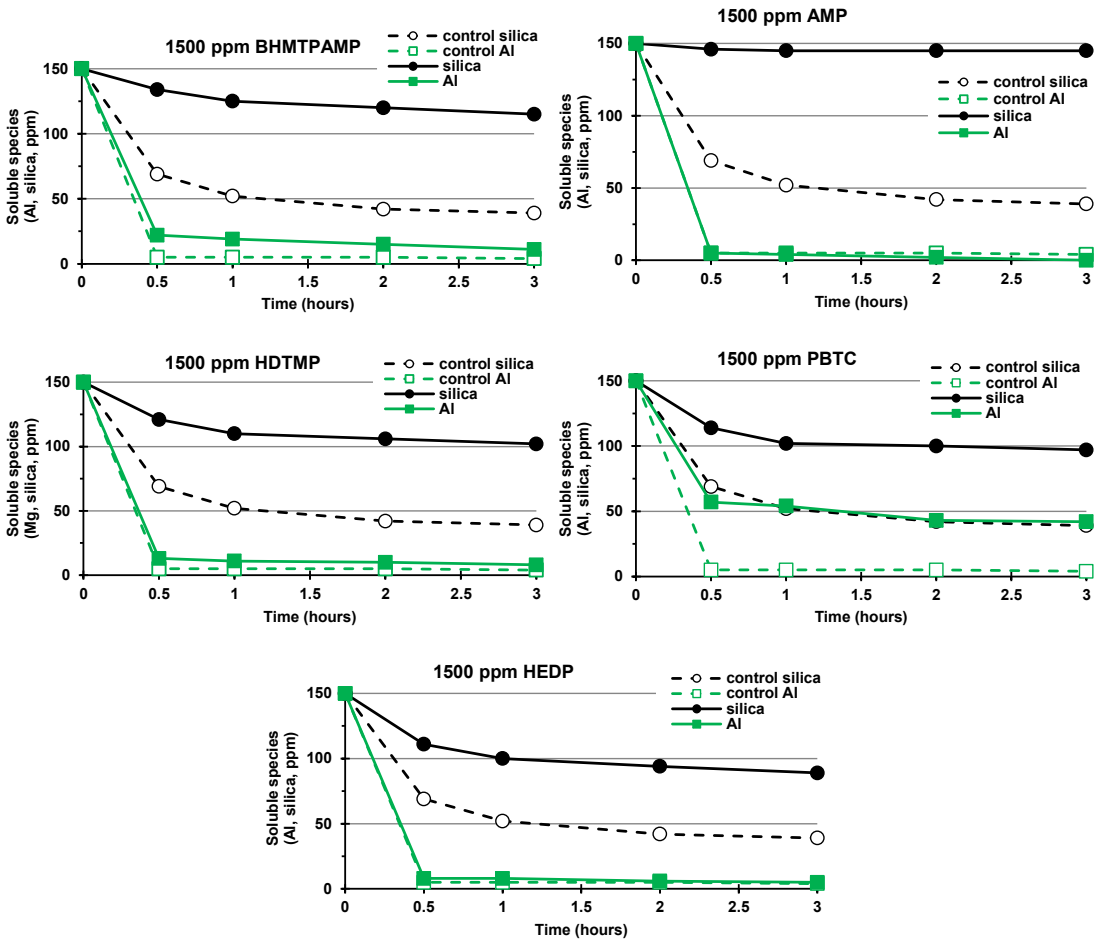

Figure 7: Simultaneous stabilization of Al^{3+} and silicate, in the presence of 1500 ppm of phosphonate inhibitors.

Table 2: Silica (ΔSilica) splits for all inhibitors present in the "aluminum silicate" system after 3 hours of precipitation time[a]

Inhibitor dosage (ppm)	ΔSilica, ppm				
	PBTC	**HEDP**	**AMP**	**HDTMP**	**BHMTPAMP**
50	19	18	11	13	11
1500	58	50	106	63	76
	ΔAl, ppm				
	PBTC	**HEDP**	**AMP**	**HDTMP**	**BHMTPAMP**
50	1	1	1	2	1
1500	38	1	0	4	7

[a] The term "split" is defined as the actual measurement of silica or Al^{3+} (in ppm) after subtraction of the "control" value.

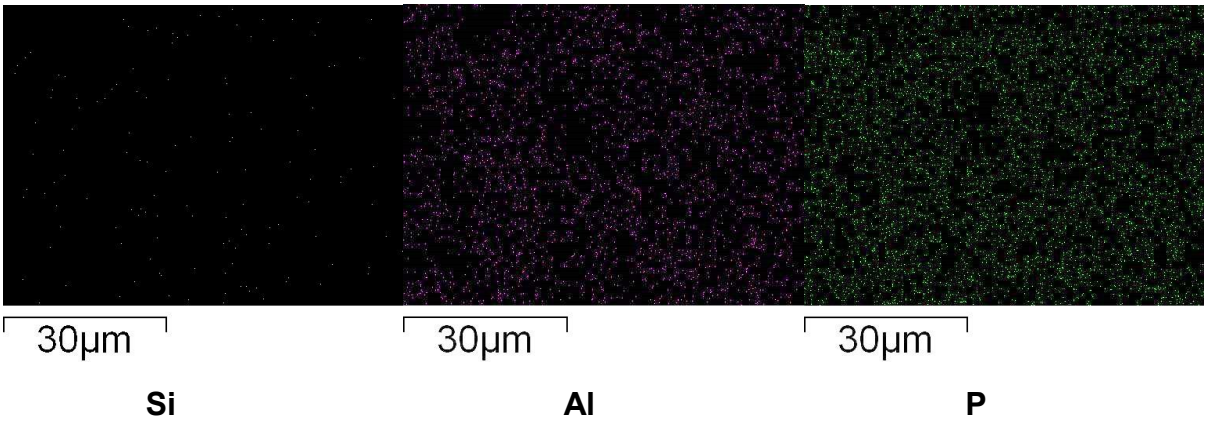

Figure 8: Elemental mapping of "aluminum silicate" precipitates in the presence of 1500 ppm HDTMP inhibitor.

4. DISCUSSION

An important issue in the control of "magnesium silicate" is the correlation between the ability of each phosphonate to stabilize Mg^{2+} ions and its affinity for Mg^{2+} ions in solution. Metal-ligand affinity is quantified by the stability constant. The aforementioned correlation is displayed in Figure 9, where the amount of Mg^{2+} ions stabilized have been plotted against relevant Mg-phosphonate stability constants. Mg-phosphonate stability constants were taken from the literature for HEDP (Foti *et al.* 2013), HDTMP (Dequest), AMP (Sawada *et al.* 2000), and diethylenetriamine-N,N,N′,N″,N″-pentakis(methylenephosphonic acid) (a similar pentaphosphonate to BHMTPAMP) (Cigala *et al.* 2014). Unfortunately, no stability constant is available for PBTC. It is clearly seen that the higher the Mg-phosphonate stability constant is, the higher the amount of Mg^{2+} ions stabilized by the phosphonate inhibitor. This is a reflection of the affinity of each phosphonate additive for Mg^{2+}, and hence the stability of the produced complex in solution.

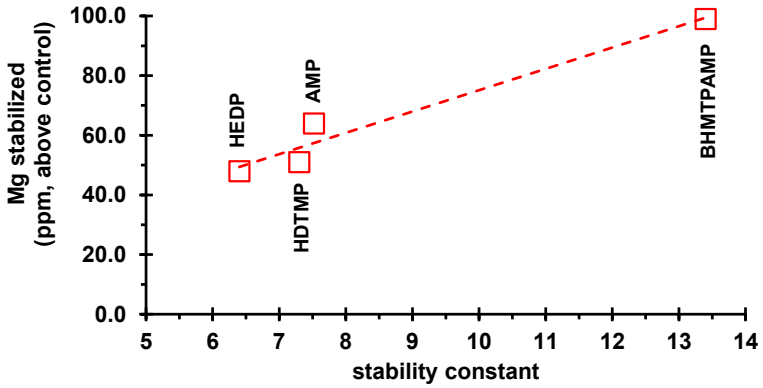

Figure 9: Correlation between stabilization of Mg^{2+} ions stabilized by phosphonate inhibitors and corresponding Mg-phosphonate stability constants.

Unfortunately, similar data on stability constants for Al^{3+} and phosphonates are not readily available for the phosphonates studied here (principally due to the insolubility of Al-phosphonate complexes (Lacour *et al.* 1998)), so similar correlations cannot be safely drawn for the stabilization of "aluminum silicate". However, it is reasonable to assume that such correlations may exist in the chelation of Al^{3+} by the phosphonate additives.

The "Al^{3+}-silicate-phosphonate" system is much more complex than the corresponding "Mg^{2+}-silicate-phosphonate" system. At pH = 7.0 there is high propensity of Al^{3+} to precipitate as $Al(OH)_3$ (Tokoro *et al.* 2014). Therefore, the following competitive processes take place simultaneously in the "Al^{3+}-silicate-phosphonate" system:

(a) Speciation of Al^{3+} as aqua and hydroxyl complexes at pH = 7.0
(b) Precipitation of $Al(OH)_3$
(c) Formation and precipitation of "aluminum silicate"
(d) Formation of soluble "aluminum-phosphonate" complexes
(e) Formation and precipitation of insoluble "aluminum-phosphonate" complexes
(f) Loss of Al^{3+}, either absorbed onto, or incorporated into, silica precipitates

Hence, a much more thorough study of the behavior of Al^{3+} in the presence of silicate is needed, in order to delineate whether Al^{3+} actually catalyzes the silicate polycondensation reaction, or $Al(OH)_3$ particles provide an appropriate, hydroxylated surface for silicic acid to polymerize into colloidal silica particles attached on the $Al(OH)_3$ surface.

5. CONCLUSIONS

Herein, we presented an attempt to study the effect of a variety of antiscalant phosphonate additives on the inhibition of silica formation in the presence Mg^{2+} or Al^{3+} ions. The conclusions reached are:

(1) All phosphonate antiscalants demonstrate variable stabilization effectiveness for molybdate-reactive silica (silicic acid) in the presence of Mg^{2+} or Al^{3+} ions.
(2) The inhibition efficiency of phosphonates, quantified by ΔSilica (see Table 1), generally increases with inhibitor concentration.
(3) The phosphonate additives act as chelators/ligands for Mg^{2+} ions, and thus they turn off its catalytic effect in silicic acid polycondensation. A similar effect can be postulated for Al^{3+}.
(4) The silica precipitates that form in the presence of Mg^{2+} or Al^{3+} ions are Mg-, or Al-absorbed amorphous silica, with variable Mg and Al contents.
(5) Limited phosphonate entrapment into the precipitates occurs due to formation of sparingly-soluble Mg- or Al-phosphonate "complexes" that are found in the precipitated solids (based on elemental analyses of phosphorus).
(6) Ranking of phosphonate-type inhibitors is different for the two "metal silicate" (Mg and Al) types investigated.

REFERENCES

Arata, E., Erich, R., and Paradis, R.: Recent Innovations in Pigging Technology for the Removal of Hard Scale From Geothermal Pipelines, Proceedings, 20th Annual PNOC-EDC Geothermal Conference, 1999, p. 123.

Browne, B.A., and Driscoll, C.T.: Soluble Aluminum Silicates: Stoichiometry, Stability, and Implications for Environmental Geochemistry, Science, 256, (1992), 1667-1670.

Canizares, P., Martínez, F., Jiménez, C., Lobato, J., and Rodrigo, M.A.: Comparison of the Aluminum Speciation in Chemical and Electrochemical Dosing Processes, Ind. Eng. Chem. Res., 45, (2006), 8749-8756.

Cigala, R.M., Cordaro, M., Crea, F., De Stefano, C., Fracassetti, V., Marchesi, M., Milea, M., and Sammartano, S.: Acid–Base Properties and Alkali and Alkaline Earth Metal Complex Formation in Aqueous Solution of Diethylenetriamine-N,N,N′,N″,N″-pentakis(methylenephosphonic acid) Obtained by an Efficient Synthetic Procedure. Ind. Eng. Chem. Res., 53, (2014), 9544–9553.

Demadis, K.D., Ketsetzi, A., and Sarigiannidou, E.-M.: Catalytic Effect of Magnesium Ions on Silicic Acid Polycondensation and Inhibition Strategies Based on Chelation, Ind. Eng. Chem. Res., 51, (2012), 9032-9040.

Demadis, K.D.: Recent Developments in Controlling Silica and Magnesium Silicate in Industrial Water Systems, in Science and Technology of Industrial Water Treatment; CRC Press, London (2010) Chapter 10, pp. 179-203.

Demadis, K.D.: Water Treatment's "Gordian Knot", Chem. Processing, 66(5), (2003) 29-32.

Dequest® 2040, 2050 and 2060 product series, http://www.dequest.com.

Deutscher, S.B., Ross, D.M., Quong, R., and Harrar, J.E.: Studies of the Dissolution of Geothermal Scale, Lawrence Livermore Laboratory Report UCRL-52897 (Livermore, CA: 1980).

Eaton, A.D., Clesceri, L.S., Rice, E.W., Greenberg, A.E., and Franson, M.H.: Standard Methods for Examination of Water & Wastewater (Washington, DC: American Public Health Association, 2012).

Foti, C., Giuffrè, O., and Sammartano, S.: Thermodynamics of HEDPA Protonation in Different Media and Complex Formation With Mg2+ and Ca2+, J. Chem. Thermodyn., 66, (2013), 151-160.

Gallup, D.L., and von Hirtz, P.: Control of Silica-Based Scales in Cooling and Geothermal systems, in Mineral scales and deposits: Scientific and technological approaches. Elsevier, Amsterdam (2015) Chapter 22, pp. 573-582.

Gallup, D.L.: Aluminum Silicate Scale Formation and Inhibition (2): Scale Solubilities and Laboratory and Field Inhibition Tests, Geothermics, 27, (1998), 485-501.

Gallup, D.L.: Aluminum Silicate Scale Formation and Inhibition: Scale Characterization and Laboratory Experiments, Geothermics, 26, (1997), 483-499.

Gallup, D.L.: Brine pH Modifcation Scale Control Technology, Geoth. Res. T., 20, (1996), 749-755.

Hater, W., zum Kolk, C., Braun, G., and Jaworski, J.: The Performance of Anti-Scalants on Silica-Scaling in Reverse Osmosis Plants, Des.Wat. Treat., 51, (2013), 908-914.

Hater, W., zum Kolk, C., Dupoiron, C., Braun, G., Harrer, T., and Götz, T.: Silica Scaling on Reverse Osmosis Membranes — Investigation and New Test Methods, Des.Wat. Treat., 31, (2011) 326-330.

Henley, R.W.: pH and Silica Scaling Control in Geothermal Field Development, Geothermics, 12, (1983), 307-321.

Icopini, G.A., Brantley, S.L., and Heaney, P.J.: Kinetics of Silica Oligomerization and Nanocolloid Formation as a Function of pH and Ionic Strength at 25 °C, Geochim.Cosmochim. Acta, 69, (2005), 293-303.

Ketsetzi, A., Stathoulopoulou, A., and Demadis, K.D.: Being "Green" in Chemical Water Treatment Technologies: Issues, Challenges and Developments, Desalination, 223, (2008), 487-493.

Kristmanndóttir, H., Ólafsson, M., and Thórhallsson, S.: Magnesium Silicate Scaling in District Heating Systems in Iceland, Geothermics, 18, (1989), 191-198.

Kristmannsdottir, H.: Types of Scaling Occurring by Geothermal Utilization in Iceland, Geothermics, 18, (1989), 183-190.

Lacour, S., Deluchat, V., Bollinger, J.-C., and Serpaud, B.: Complexation of Trivalent Cations (Al(III), Cr(III), Fe(III)) With Two Phosphonic Acids in the pH Range of Fresh Waters, Talanta, 46, (1998), 999-1009.

Mavredaki, E., Neofotistou, E., and Demadis, K.D.: Inhibition and Dissolution as Dual Mitigation Approaches for Colloidal Silica (SiO2) Fouling and Deposition in Process Water Systems: Functional Synergies, Ind. Eng. Chem. Res., 44, (2005), 7019-7026.

Messer, P.H., Pye, D.S., and Gallus, J.P.: Injectivity Restoration of a Hot-Brine Geothermal Injection Well, J. Pet. Tech., 30, (1978), 1225-1230.

Neofotistou, E., and Demadis, K.D.: Silica Scale Growth Inhibition by Polyaminoamide STARBURST® Dendrimers, Colloids Surf. A, 242, (2004), 213-216.

Perry, C.C., and Shafran, K.L.: The Systematic Study of Aluminium Speciation in Medium Concentrated Aqueous Solutions, J. Inorg. Biochem., 87, (2001), 115-124.

Preari, M., Spinde, K., Lazic, J., Brunner, E., and Demadis, K.D.: Bioinspired Insights Into Silicic Acid Stabilization Mechanisms: The Dominant Role of Polyethylene Glycol-Induced Hydrogen Bonding, J. Am. Chem. Soc., 136, (2014), 4236-4244.

Rothbaum, H.P., Anderton, B.H., Harrison, R.F., Rohde, A.G., and Slatter, A.: Effect of Silica Polymerisation and pH on Geothermal Scaling, Geothermics, 8, (1979), 1-20.

Sawada, K., Duan, W., Ono, M., and Satoha, K.: Stability and Structure of Nitrilo(acetate–methylphosphonate) Complexes of the Alkaline-Earth and Divalent Transition Metal Ions in Aqueous Solution, J. Chem. Soc. Dalton Trans., (2000), 919-924.

Shull, K.E., and Guthan, G.R.: Rapid Modified Eriochrome Cyanine R Method for Determination of Aluminum in Water, J. Am. Water Works Assoc. 59, (1967), 1456-1468

Spinthaki, A., Petratos, G., Matheis, J., Hater, W., and Demadis, K.D.: The Precipitation of "Magnesium Silicate" Under Geothermal Stresses: Formation and Characterization, Geothermics, 74, (2018), 172-180.

Stathoulopoulou, A., and Demadis, K.D.: Enhancement of Silicate Solubility by Use of "Green" Additives: Linking Green Chemistry and Chemical Water Treatment, Desalination, 224, (2008), 223-230.

Tokoro, C., Suzuki, S., Haraguchi, D., and Izawa, S.: Silicate Removal in Aluminum Hydroxide Co-Precipitation Process, Materials, 7, (2014), 1084-1096.

Topçu, G., Çelik, A., Baba, A., and Demir, M.M.: "Design of Polymeric Antiscalants Based on Functional Vinyl Monomers for (Fe, Mg) Silicates, Energy Fuels, 31, (2017), 8489-8496.

Truesdale, V.W., Smith, P.J., and Smith, C.J.: Kinetics of α- and β-Molybdosilicic Acid Formation, Analyst, (1979), 897-918.

Yokoyama, T., Sato, Y., Maeda, Y., Tarutani, T., and Itoi, R.: Siliceous Deposits Formed From Geothermal Water I. The Major Constituents and the Existing States of Iron and Aluminum, Geothermal J., 27, (1993), 375-384.

Young, P.R.: Magnesium Silicate Precipitation, Proceedings, CORROSION 1993 Paper no. 466 (Houston, TX: NACE 1993).